Formation of structure of TiNiCu alloys with high copper content upon producing by planar flow casting

Formation of structure of TiNiCu alloys with high copper content upon producing by planar flow casting

A V Shelyakov, O N Sevryukov, N N Sitnikov, K A Borodako, I A Khabibullina

National Research Nuclear University MEPhI (Moscow Engineering Physics Institute), Kashirskoe sh. 31, 115409 Moscow, Russia

E-mail: AVShelyakov@mephi.ru

Abstract. The rapidly quenched alloys of the quasibinary intermetallic TiNi-TiCu system with a high copper content (more than 25 at.%) are of great interest as shape memory materials due to the possibility of a significant decrease in the temperature and deformation hysteresis in comparison with the binary TiNi alloy. To obtain alloys with a copper content of 25 to 40 at.%, the planar flow casting technique was used. The alloys were fabricated at a melt cooling rate of about 10^6 K/s in the form of ribbons 30–50 μm thick and wide in the range from 7 to 20 mm. The study of the structure of the alloys was carried out using X-ray diffraction analysis, scanning and transmission electron microscopy. It was shown that from the ribbon side, contacting the quenching wheel, all alloys are amorphous, while on the non-contact side of the ribbons of alloys with 25 and 30 at.% Cu, a thin surface crystalline layer with a B2 structure is observed. Using energy dispersive X-ray spectroscopy, it was found that the content of the alloy components in the amorphous and crystalline phases coincides.

1. Introduction

TiNi-based alloys occupy a special place among materials with a shape memory effect (SME). These alloys have found wide and effective application in such fields of technology as space technology, biomedicine, robotics, and MEMS due to a large value of reversible deformation and a high ratio of generated forces to weight and size characteristics during the implementation of the SME [1, 2].

The addition of a third alloying element (Cu, Fe, Al, Hf, etc.) to a TiNi alloy near to the equiatomic composition can noticeably change the characteristics of the SME. In particular, alloys of the quasi-binary intermetallic TiNi–TiCu system are characterized not only by high values of the SME parameters, but also attract attention due to the possibility of significantly reducing the temperature and deformation hysteresis in comparison with the binary TiNi alloy [3]. However, the production of alloys of the TiNi – TiCu system with a copper content of more than 10 at.% by standard methods of casting or sintering can lead to formation of undesirable Ti–Cu phases, which embrittle the alloys and prevent the manifestation of the SME. This problem can be solved using ultrarapid liquid quenching technology (melt spinning or planar flow casting techniques) [4, 5]. A feature of TiNi – TiCu alloys with a high copper content (more than 20 at.%) is that at high cooling rates (about 10^6 K/s) they can be obtained in the amorphous state in the form of thin ribbons with uniform chemical composition [6, 7]. A heat treatment of the amorphous alloys results in a pronounced SME, whose parameters are largely determined by the structural properties of alloys in the initial state after quenching [8–12].

The aim of this work was to study the structure formation processes in rapidly quenched TiNiCu alloys with a copper content of more than 25 at.% obtained by planar flow casting.

2. Experimental

2.1. Samples

The technological process for producing the alloys of the TiNi-TiCu quasibinary system by planar flow casting included the preparation of ingots of alloys from ultrapure metals with sixfold remelting in an arc furnace in an argon atmosphere, subsequent melting in a quartz crucible in a helium atmosphere, and extrusion of the melt through a narrow nozzle in the crucible onto the surface of a rapidly rotating copper wheel. To obtain ribbons up to 20 mm wide, the slotted nozzle of 0.4 mm wide was used, and the distance between the nozzle edge and the wheel surface was 0.4-0.6 mm. Since to produce the alloys in the amorphous state, it is necessary that the temperature of the ribbon before separation from the quenching wheel did not exceed the glass transition temperature, the time of contact of the ribbon with the wheel was increased by keeping it on the wheel until almost full completion of the wheel turn and ribbon separation from the wheel by means of a special removable device. The cooling rate of the melt was about 10^6 K/s for all alloys. Using the planar flow casting, the alloys of the TiNi-TiCu quasibinary system with copper content from 25 to 40 at.% were obtained in the form of ribbons 30–50 μm thick and wide in the range from 7 to 20 mm. Besides, an additional alloying of the alloys with aluminum, which, as is known, increases the casting properties and promotes amorphization of the alloys, was carried out. For detailed study, the TiNiCu alloys with a copper content of 25, 30, 35, and 40 at. % (hereinafter referred to as 25Cu, 30Cu, 35Cu and 40Cu, respectively, Table 1), as well as the 25Cu alloy with the addition of 0.6 at.% Al (0.6Al) were selected.

Table 1. Compositions of the alloys of the TiNi – TiCu system and their notations.

Alloy	25Cu	30Cu	35Cu	40Cu	0.6Al
Composition (at.%)	$Ti_{50.2}Ni_{24.8}Cu_{25}$	$Ti_{50.2}Ni_{19.8}Cu_{30}$	$Ti_{50.2}Ni_{14.8}Cu_{35}$	$Ti_{50.2}Ni_{9.8}Cu_{40}$	$Ti_{50.2}Ni_{24.8}Cu_{24.4}Al_{0.6}$

2.2. Techniques

The structure of the obtained alloys was studied by metallography, electron microscopy, and X-ray diffraction analysis. For metallographic research of ribbon samples, their cross-sections were made using Buehler equipment. The last stage of polishing was carried out using an acid-containing mixed suspension with an abrasive grain size of 50 nm. The cross-sectional microstructure of the samples was investigated using FEI Quanta 600 FEG scanning electron microscope (SEM). The fine structure of the alloys was studied using JEOL JEM 2100 high-resolution transmission electron microscope (TEM). X-ray diffraction analysis was performed by Bragg-Brentano focusing on PANalytical Empyrean diffractometer in CuK_α radiation.

3. Results and Discussion

Electron microscopic studies of the cross section of the ribbons revealed a difference in structure from the contact (facing the quenching wheel) and the non-contact (free) side of the ribbons (Fig. 1). An amorphous structure is observed in all the ribbons; however, a thin crystalline layer with a thickness of about 3.5 and 1.5 μm was found on the free surface of ribbons of 25Cu and 30Cu alloys, respectively (Fig. 1a, b). As we showed earlier [13], this is due to the different cooling rates of the melt on the contact and free surfaces of the ribbon, when the cooling rate on the free surface is insufficient for amorphization of the alloy. At the same time, a crystalline layer is not observed on the free surface of ribbons of 35Cu, 40Cu, and 0.6Al alloys (Fig. 1c, d). Furthermore, in the 25Cu and 30Cu alloys, individual crystalline inclusions were revealed in the amorphous matrix (indicated by the arrow in Fig. 1e), which were practically absent at the beginning of the ribbons and were found mainly at the end of

the ribbons. This, obviously, is associated with a certain decrease in the cooling rate of the melt at the end of the quenching process due to its technological features, mainly due to a decrease in the temperature of the melt, as well as an increase in the temperature on the surface of the quenching wheel in the zone of formation of the ribbon.

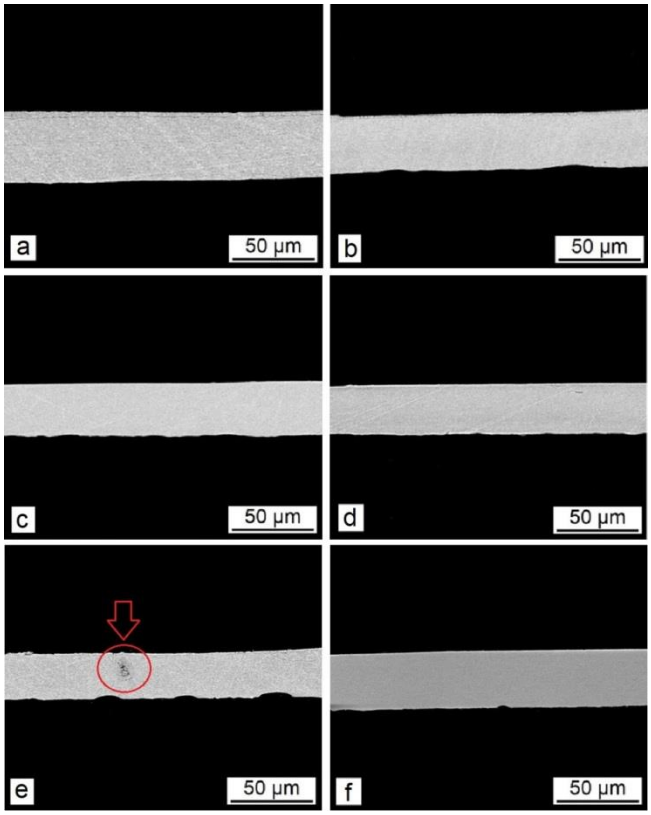

Figure 1. SEM images of typical cross sections of rapidly quenched ribbons of the alloys of the TiNi-TiCu system: 25Cu (a), 30Cu (b, e), 35Cu (c), 40Cu (d) and 0.6Al (f).

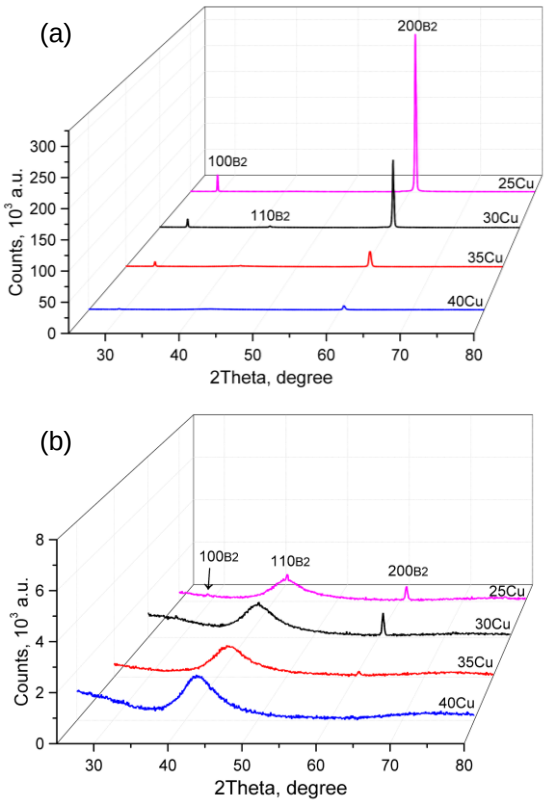

Figure 2. X-ray diffraction patterns obtained from the free (a) and contact (b) surfaces of rapidly quenched ribbons of the alloys of the TiNi-TiCu system at room temperature.

The phase composition of the alloys was determined using x-ray diffraction analysis from the contact and free sides of the ribbons (Fig. 2). The diffraction patterns of the free surface of ribbons of 25Cu and 30Cu alloys at room temperature (Fig. 2a) show pronounced diffraction peaks of the B2 austenitic phase (CsCl type), which is due to the presence of a surface crystalline layer (Fig. 1a, b). The peaks of $(200)_{B2}$ and $(100)_{B2}$ are of the highest intensity, which is not typical for the bcc lattice of B2-phase and indicates the texture of the formed crystalline layer. With an increase in copper content up to 40 at.% the intensity of reflections sharply decreases; this is associated with the disappearance of the surface crystalline layer (Fig. 1c, d). At the same time, diffractograms from the contact side of all the ribbons show a broad halo near $2\theta = 42$ degrees (Fig. 2b), which indicates the amorphous state of the alloys; however, small peaks of the B2 phase (hundreds of times lower intensity compared with the free side) are observed in the samples of 25Cu and 30Cu alloys, which confirms the presence of a small fraction of crystallites in the amorphous matrix, since the surface crystalline layer on the contact side is not found (Fig. 1a, b, e). It is noteworthy that in the 0.6Al alloy, no structural peaks were detected both from the contact and from the free side of the ribbon (Fig. 3a).

Thus, an increase in the copper content of more than 30 at.% as well as alloying with aluminum (0.6 at.%) leads to complete amorphization of the TiNi-TiCu system alloys. It should be noted that the

obtained microstructure is noticeably different from the microstructure of alloys of the same composition made by melt spinning (MS). In particular, the presence of the B19 (orthorhombic) martensitic phase was detected in the MS alloy with 25 at.% Cu, while in the MS alloys with 30–40 at.% Cu, both structural peaks in the diffraction patterns and the surface crystalline layer were completely absent [14].

The TEM study of the fine structure made it possible to reveal in all alloy samples the ultrafine absorption contrast which is typical for the amorphous phase. In the corresponding electron diffraction patterns, a series of diffuse rings with decreasing intensity was observed as the angle of the diffraction vector increased. Typical bright-field TEM image and microelectron diffraction pattern for 0.6Al alloy are presented in Figure 3b.

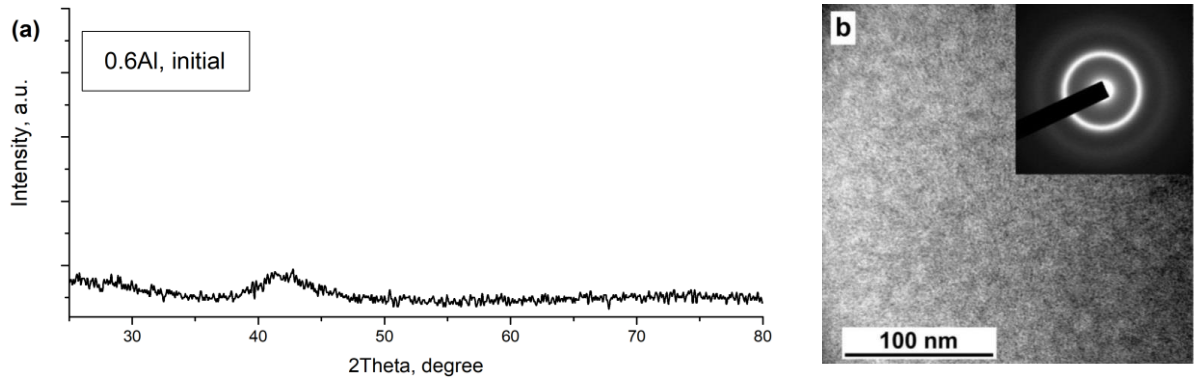

Figure 3. X-ray diffraction pattern (a) and bright-field TEM image with the corresponding microelectron diffraction pattern (b) for 0.6Al alloy.

For elemental analysis of alloys, the method of energy dispersive X-ray spectroscopy (EDS) was used in SEM studies of the cross section of ribbons. It was found that in the region of the amorphous state the elemental composition for all studied alloys corresponds to the composition of the initial ingot within the accuracy of the method. A typical view of the selected region of the 35Cu alloy ribbon is shown in Fig. 4a, and the corresponding content of each of the components (Ti, Ni, and Cu) is presented in Table 2 (Spectrum 1). Special attention was paid to comparing the chemical composition of the amorphous matrix, the surface crystalline layer, and individual crystallites in the bulk of the ribbon where they are present. Figure 4 b, c shows the corresponding regions of study of a 25Cu alloy ribbon. As can be seen, the content of the alloy components in the amorphous and crystalline phases coincides (Table 2, Spectra 2-5).

The results obtained confirm the fact that the reason for the formation of the surface crystalline layer is the different rates of solidification of the free and contact ribbon surfaces but not the difference between the chemical composition of the alloy in the ribbon volume and its surface layer.

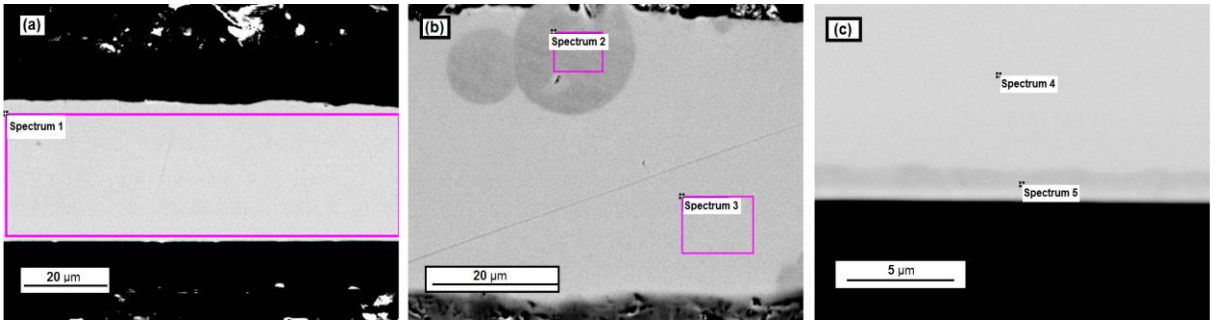

Figure 4. Determination of the elemental composition of alloys 35Cu (a) and 25Cu (b, c) by the EDS method.

Table 2. Composition of the TiNiCu alloys determined by the EDS method.

Element (at.%)	Spectrum 1	Spectrum 2	Spectrum 3	Spectrum 4	Spectrum 5
Ti	50.44	50.58	50.40	50.69	50.57
Ni	14.67	24.85	24.86	24.71	24.62
Cu	34.89	24.57	24.74	24.60	24.81

4. Conclusions

We used the planar flow casting technique to produce alloys of the quasibinary TiNi-TiCu system with a copper content of 25 to 40 at.% in the form of thin (30–50 μm) ribbons with an increased width (7–20 mm) compared to ribbons obtained by melt spinning technique. The study of the structure and elemental composition of the alloys allowed us to draw the following conclusions:

1) the alloys with 25 and 30 at.% Cu forms an amorphous-crystalline structure with a thin (1.5–3.5 μm) crystalline layer on the surface of the ribbons having the structure of the austenite phase B2;

2) the chemical composition of the alloys in the amorphous and crystalline phases is the same and corresponds to the composition of the initial ingot, so the reason for the formation of the surface crystalline layer is the different rates of solidification of the free and contact ribbon surfaces;

3) the increase in the copper content of more than 30 at.% as well as alloying with aluminum (0.6 at.%) leads to complete amorphization of the TiNi-TiCu system alloys.

Acknowledgments

The study was carried out at the expense of a grant from the Russian Science Foundation (Project No. 19-12-00327).

References

[1] Kohl M, Ossmer H, Gueltig M and Megnin C 2018 *Shape Mem. Superelasticity* **4** 127
[2] Jani J M, Leary M, Subic A and Gibson M A 2014 *Mater. Design* **56** 1078
[3] Morgiel J, Cesari E, Pons J, Pasko A and Dutkiewicz J J 2002 *Mater. Sci.* **37** 5319
[4] Shelyakov A V, Sitnikov N N, Menushenkov A P, Koledov V V and Irjak A I 2011 *Thin Solid Films* **519** 5314
[5] Kang S W, Lim Y M, Lee Y H, Moon H J, Kim J W and Nam T H 2010 *Scr. Mater.* **62** 71
[6] Schlossmacher P, Boucharat N, Wilde G, Roesner H and Shelyakov A V 2003 *J. Phys. IV France* **112** 731
[7] Shelyakov A V, Sitnikov N N, Menushenkov A P, Korneev A A, Rizakhanov R N and Sokolova N A 2013 *J. Alloys Compd.* **577** S251
[8] Chang S H, Wu S K and Kimura H 2007 *Intermetallics* 15 233
[9] Schlossmacher P, Rösner H, Shelyakov A V and Glezer A M 2000 *Mater. Sci. Forum* **327-328** 131
[10] Potapov P L, Kulkova S E, Shelyakov A V, Okutsu K, Miyazaki S and Schryvers D 2003 *J. Phys. IV France* **112** 727
[11] Tong Y X, Liu Y and Xie Z L 2008 *J. Alloys Compd.* **456** 170.
[12] Chen C H, Wang H K and Wu S K 2018 *Intermetallics* **93** 347
[13] Shelyakov A V, Sitnikov N N, Menushenkov A P, Rizakhanov R N and Ashmarin A A 2015 *Bull. Russ. Acad. Sci. Phys.* **79** 1281.
[14] Sitnikov N N, Shelyakov A V, Khabibullina I A, Mitina N A and Resnina N N 2018 *Inorg. Mater.: Appl. Res.* **9(2)** 279